Hybrid grab concepts for varying operational conditions

Tessa Virginia van Kol

Additional details regarding the research results are provided in the appendices

Confidential

Hybrid grab concepts for varying operational conditions

By

Tessa Virginia van Kol

Master Thesis

in partial fulfilment of the requirements for the degree of

Master of Science
in Mechanical Engineering

at the Department Maritime and Transport Technology of Faculty Mechanical, Maritime and Materials Engineering of Delft University of Technology
to be defended publicly on Tuesday July 13, 2021 at 11:00 AM

Student number:	4628586	
MSc track:	Multi-Machine Engineering	
Report number:	2021.MME.8519	
Confidential:	Yes	
Supervisors:	Dr. M.J. Mohajeri	Post Doctoral Researcher TU Delft
	Dr. J. Jovanova	Assistant Professor TU Delft
	Dr. ir. D.L. Schott	Associate professor TU Delft
	Ir. W.A. de Kluijver	Nemag B.V.
Thesis committee:	Dr. ir. D.L. Schott,	TU Delft committee Chair, Faculty
	Dr. ir. M. Langelaar,	TU Delft committee member, Faculty
Date:	July 13, 2021	

TU Delft

Hybrid Grab Concepts for Varying Operational Conditions

Tessa V. van Kol
Department of Maritime and Transport Technology
Delft University of Technology
T.V.vanKol@student.tudelft.nl

M. Javad Mohajeri
Department of Maritime and Transport Technology
Delft University of Technology
M.Mohajeri-1@tudelft.nl

Jovana Jovanova
Department of Maritime and Transport Technology
Delft University of Technology
J.Jovanova@tudelft.nl

Dingena L. Schott
Department of Maritime and Transport Technology
Delft University of Technology
D.L.Schott@tudelft.nl

Wilbert A. de Kluijver
Nemag
Wilbert.deKluijver@nemag.com

Michel Corbeau
Nemag
Michel.Corbeau@nemag.com

***Abstract*—Grabs are a essential link within the intercontinental transport of bulk material such as iron ore. Grabs are used to unload the moored bulk carriers in reliable and efficient way. During the unloading process varying operational conditions influence the grab performance negatively, i.e. variable amount of material being grabbed at each cycle leading to under- or overperfomance of the grab. The current grab design is fixed against these varying operational conditions. To enhance the grab design, an additional closing mechanism that can maximize the payload with the possibility to reach a consistent payload is investigated. A grab design combining the mechanical (rope) closing mechanism with an additional closing mechanism for providing an extra penetration force when needed is termed as a hybrid grab. The investigation showed promising hybrid concepts that used various mechanism to create a variable and controllable torque. Back-of-the-envelope calculations or or by testing the hybrid grab concept in the co-simulation MBD-DEM environment the performance in relation to the desired torque function was approximated. The NX grab compression spring concept is the most promising concept regarding the desired torque function, performance on the define KPIs and is more advanced in the design process. By investigating and developing hybrid grab concepts, the grab design can become one step closer towards "smart" grab designs.**

Keywords: **Hybrid grab, varying operational conditions, DEM**

I. Introduction

Intercontinental transportation of bulk materials such as iron ore is primarily accomplished by bulk carriers. Upon arrival at the destination terminals, bulk carriers are commonly unloaded by grabs as shown by Figure 1.During unloading of a bulk carrier, grabs collect the bulk material from the cargo hold to transfer toward the next bulk handling equipment, commonly employed by hopper-conveyor system, from where it will be further transported into the terminal.

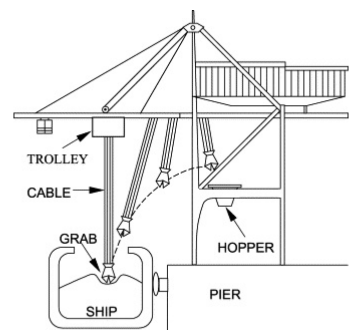

Fig. 1. Unloading process of a bulk carrier by a grab attached to a gantry crane [1]

The unloading process faces many challenges including varying operational conditions and grab design restrictions that result in a deviation from the nominal grab performance. The varying operational conditions include bulk material properties, human operators and interaction with other bulk handling equipment. Improvements of the grab design are required to reach a maximized consistent payload. Recent studies towards developing grabs showed improvements of the grab; resulting in an increased unloading capacity with respect to the previous design of the grab [2]–[4].

However, the optimized grab design still showed some inconsistency in payload as the grab design is fixed against varying operational conditions. This research seeks to enhance the grab design with an additional closing mechanism that can maximize the payload with the possibility to reach a consistent payload, thus, increasing the efficiency of the unloading operation. A grab design combining the mechanical (rope) closing mechanism with an additional closing mechanism for

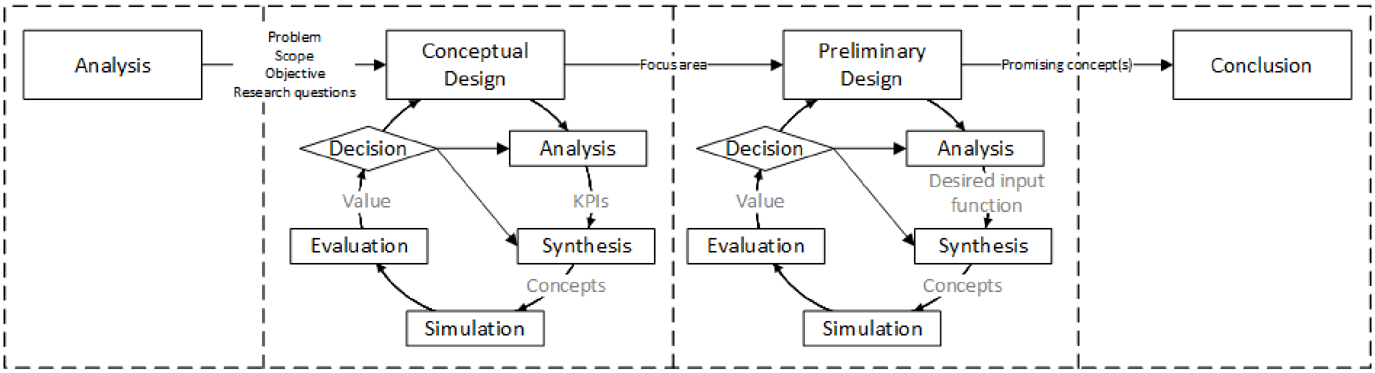

Fig. 2. Hybrid grab design strategy

providing an extra penetration force when needed is termed as a hybrid grab.

II. Method

Over the past years virtual prototyping of grabs, Lommen [5], has been developed which enabled the possibility of testing grab prototypes in a virtual environment. To model grabs in interaction with bulk a validated co-simulation between of discrete element method (DEM) and Multi-Body Dynamics (MBD) was created. Mohajeri [6] included the material model of iron ore fines in the existing co-simulation framework of Lommen [5] that can capture the cohesive and stress-history dependent behaviour. This DEM material model is selected for this research. Virtual prototyping is incorporated in the design strategy of this research for developing hybrid grab concepts. Figure 2 presents the proposed design strategy for developing hybrid grab concepts that can meet defined key performance indicators (KPIs). The phases presented in this strategy are performed sequentially in the following order: (I) Analysis, (II) Conceptual design and (III) Preliminary design and (IV) Conclusion.

During the analysis phase the problem, scope, objectives and research questions are defined which guide the activities and decisions in later phases of this research. Then, different additional closing mechanism concepts are explored in the conceptual design phase that form the initial design space of developing hybrid grab concepts. For this research the recently developed nemaX grab is selected as base design for developing hybrid grab concepts. The proposed design strategy can be applied with other types of grabs, however, the outcome may differ. By applying an iterative process consisting of analysis, synthesis, simulation, evaluation and decision, the initial design space is reduced until one type of additional closing mechanism remains. Then, alternatives can be explored of the selected additional closing mechanism in the preliminary design phase, i.e. hybrid grab concepts. Before exploring different hybrid grab concepts in the synthesis step of the preliminary design phase, the desired actuation function needs to be obtained. The hybrid grab needs to provide the possibility to maintain a consistent payload under varying operational conditions, thus, a variable and controllable actuation function is required. This actuation function states the duration and level of extra torque to apply during the grabbing process that will result in the desired grab performance. To find the desired actuation function under varying operational conditions, multi-objective optimization methods are employed. The varying operational condition that is considered is the bulk surface geometry, i.e. flat and irregular bulk surface, identified by [2] as the most significant varying operational condition. After the desired torque functions are obtained, various hybrid grab concepts are explored in the synthesis step of the preliminary design phase. The performance of the hybrid grab concepts are either quantified based on back-of-the-envelope calculation supported by literature or using the co-simulation MBD-DEM. Finally, conclusions are presented regarding the hybrid grab concepts.

III. Selecting an additional closing mechanism and simulation plan

Figure 3 shows the result of exploring possible solutions for increasing the payload of the nemaX grab through an additional closing mechanism. These possible solutions form the design space, which is presented as a mind map consisting of four categories, for developing hybrid grab concepts.

A sensitivity analysis is performed that allows for selecting type of additional closing mechanism maximizing the payload and thereby can create significant increase in the grab performance. Therefore, a representative concept of the categories (I) adding extra torque, (II) vibration and (III) excavation is chosen as shown in Figure 4. The validated co-simulation does not include Computational fluid dynamics (CFD) MBD - DEM possibility, and developing such a simulation requires resources that are not possible within this research. Therefore, the additional closing mechanism incorporating fluidization is excluded from the current simulation plan. Instead results of previous studies within the Transport, Engineering and Logistics (TEL) department of the Technical University (TU) of Delft together with other studies to estimate the performance of incorporating fluidization into the grab design.

In the first test plan, extra torque is applied to the main hing, z-axis, during the closing process of the grab. The level

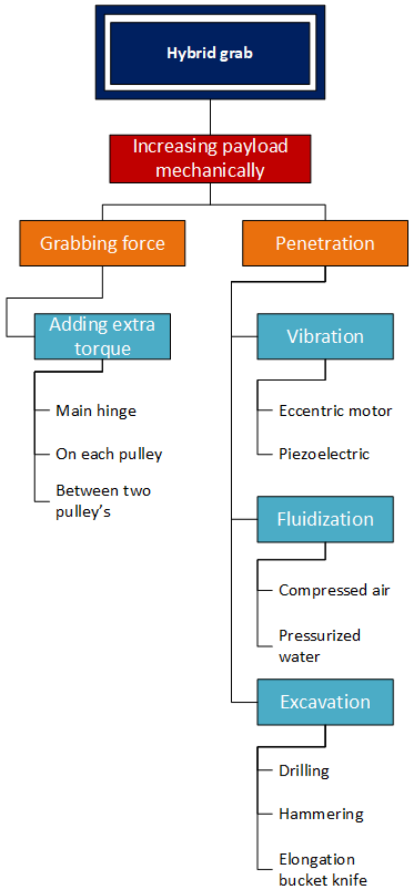

Fig. 3. Design space structured into a mind map

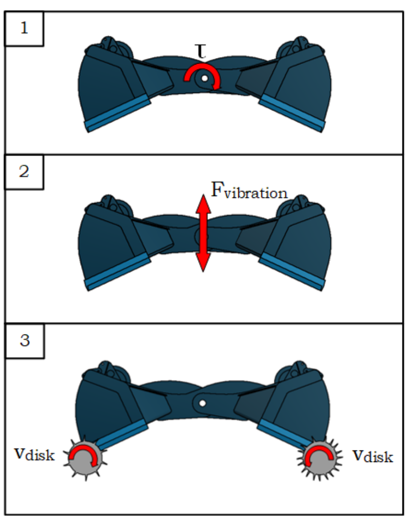

Fig. 4. Overview of test plan for selected additional closing mechanism (I) adding extra torque, (II) vibration and (III) excavation

of torque is varied from 50 kNm to 200 kNm with an interval of 50 kNm. In the second test plan, linear sinusoidal vibration is applied along the y-axis of the main hinge during the closing process of the grab. In the third test plan, four rotational disks are assembled onto the knives of the grab. The rotational velocity of the disks is varied from 1, 2.5 and 5.0 m/s. All simulations are performed on a flat bulk surface. The reference simulation with a payload of 29.98 ton is used as comparison in the following results.

IV. Results and discussion simulation plan

Figure 5 presents test plan 1 results, the payload over time for different levels of torque applied to the main hinge during the closing process of the grab. A high payload variation of 30.29 until 39.40 ton is shown. Due to the extra torque applied the grab penetrates deeper into the iron ore material, thus, resulting in an increase of payload.

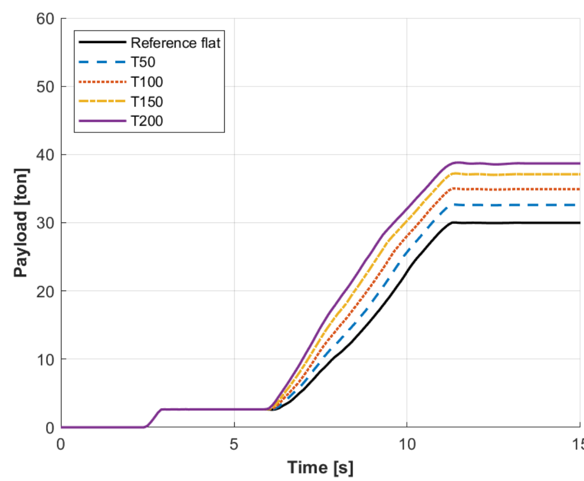

Fig. 5. Payload over time different levels of torque applied to the main hinge

Figure 6 presents test plan 2 results, the payload over time for different vibration modes, i.e. varied frequency. The increase in payload is not as significant relative to the observed payload values of test plan 1. The lowest simulated vibration frequency results is the highest increase of payload compared to the reference, whereas increasing the frequency results in approximately the same trend as the reference. Thus, when applying linear vibration on the main hinge along the y-axis low frequencies are favored. This can be explained that critical values are reached for the vibration intensity (i.e. amplitude and frequency), such that the minimum fluidization velocity, at which fluidization occurs, decreases [7]. When increasing the amplitude of low frequency vibration, it is likely to increase the payload, however, this could result in serious fatigue problems.

Figure 6 presents test plan 3 results, the payload over time for different rotational velocities of the four disks attached to the knives of the grab. The grab with rotating disk is clearly unperforming for all rotational velocities with respect

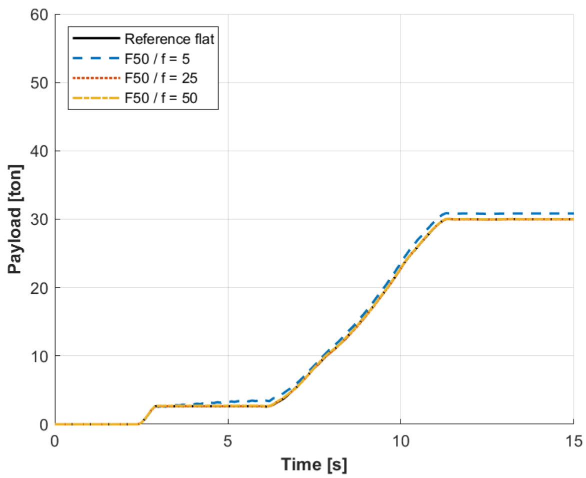

Fig. 6. Effect of linear vibration along the y-axis on the payload over time graph

to reference. Due to the compaction and cohesive properties of the iron ore material, the rotating disk fail to penetrate the material upon touchdown. Therefore, the grab is not able to grab the iron ore material resulting in a decrease of payload.

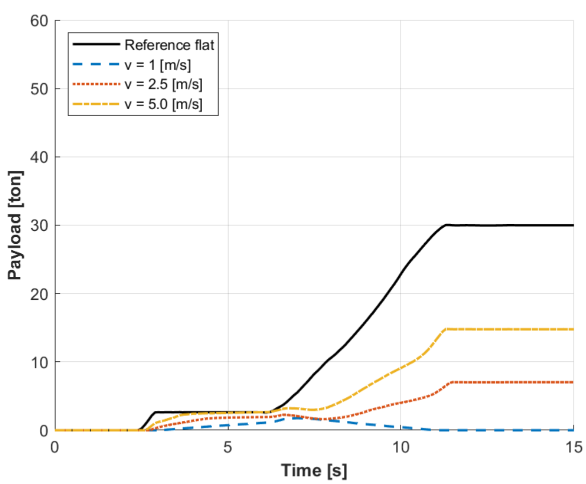

Fig. 7. Payload over time for rotating disks with different rotational velocities

A previous study by Kunne [8] investigated the concept of fluidization applied to the grab. Although he concluded that fluidization can significantly increase the initial penetration depth for free-flowing bulk material, this may not hold when applied to other (cohesive) bulk materials such as iron ore fines. In addition, implementation into practice will be difficult due to possibility of clogging of material in the nozzles used to inject compressed air into the bulk material.

Comparing all four types of additional closing mechanism, providing extra torque results in the highest increase in payload and has more advantages compared to other types of additional closing mechanism. Therefore, the design space is reduced to additional closing mechanism providing extra torque.

V. Optimization Strategy for Determining the Desired Actuation Function under Varying Operational Conditions

The response surface methodology (RSM) is employed in this research as it allows evaluating the effects of multiple input variables and their interactions between the relevant responses. Accordingly, optimization strategy based on the RSM is proposed in this research for finding the desired actuation function under varying operational conditions, i.e. two types of bulk surface geometry are considered: flat and irregular bulk surface illustrated in Figure 8. Both simulations serve as reference in the following results; with a payload of 32.85 ton for the reference flat simulation and 22.27 for the reference irregular simulation.

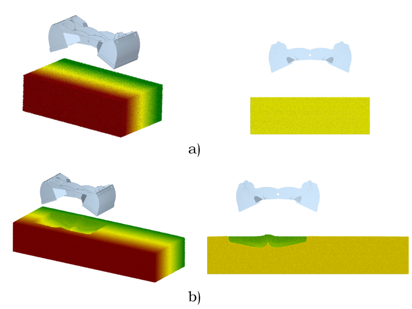

Fig. 8. a) Reference simulation (i.e. flat bulk surface), b) B0 simulation (i.e. irregular bulk surface)

Figure 9 illustrates the proposed strategy consisting of three sequential steps incorporating the steps of the RSM: (I) random sampling from design space; (II) multi-objective optimization using surrogate modelling; and (III) verifying the desired actuation function.

The Taguchi method is employed as random sampling method in step I to create a grid of distributed samples from the design space. After response data are collected, i.e. the KPIs $\psi_{payload}$, ψ_{work} and $\psi_{spillage}$, according to the samples, X, the next step is to develop a regression model for the surrogate model, f(X). In this research, four regression models are fitted to the data points and tested on their accuracy: linear regression (LR), linear support vector machine (SVM) kernel, polynomial SVM kernel and Gaussian process regression (GPR). The three KPIs are calculated according to Eq. (1)-(3):

$$\psi_{payload} = \frac{m_{DWT}}{m_{grab}} \tag{1}$$

$$\psi_{work} = \frac{W_{cable}}{W_{cable} + W_{HDP}} \tag{2}$$

$$\psi_{spillage} = \frac{m_{DWT}}{m_{DWT} + m_{spillage}} \tag{3}$$

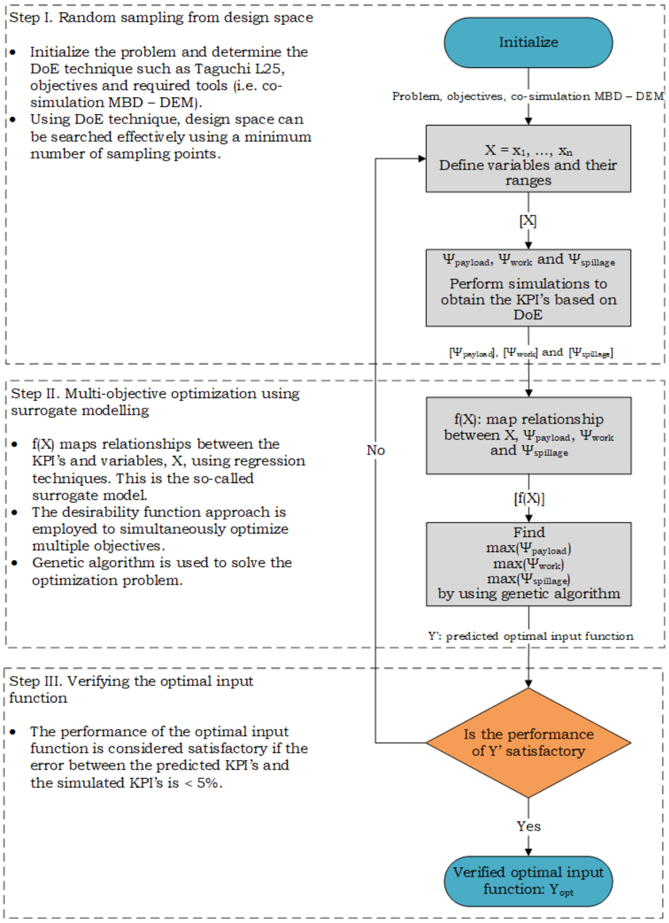

Fig. 9. Optimization strategy for finding the desired actuation function under varying operational conditions

where where m_{DWT} is the mass of the bulk solid inside the grab and m_{grab} is the mass of the grab. The W_{cable} and W_{HDP} represent the calculated work needed for the closing cables and additional closing mechanism applying the extra torque, respectively. $m_{spillage}$ is the mass spilled over the sides of the grab. Accordingly, f(X) maps relationships between the KPIs and input variables. The accuracy of the surrogate model is evaluated using the coefficient of determination, R^2, and root-mean-square error (RMSE). A minimum R^2 value of 0.80 based on [9] and a $RMSE \leq 0.12$, is considered to be met for all KPIs. To provide a more complete picture of surrogate models accuracy, additional confirmation samples are used to verify the accuracy of the surrogate models. Based on the final developed surrogate model, the specified optimization problem is solved using genetic algorithm (GA) in combination with the desirability approach [10]. Three objectives are considered in the multi-objective optimization problem: a maximized payload indicator ($\psi_{payload}$), a maximized work indicator (ψ_{work}) and a maximized spillage indicator ($\psi_{spillage}$) measured in different bulk surface geometries (i.e. flat irregular). A value of $\psi_{work} = 1$ indicates that no additional closing mechanism present to provide the torque around the main hinge (i.e. reference grab). A value of $\psi_{spillage} = 1$ indicates that no material has been spilled from the grab. All objectives are assumed to be equally important.

The absolute error is used to quantify the error between the predicted values and the actual output of the simulation. In this research, an $e \leq 5\%$ is considered an acceptable outcome during verification. The absolute error is determined according to Eq. (4):

$$e = \left| \frac{Y - Y'}{Y} \right| 100 \tag{4}$$

A. Results Desired actuation function

First, 25 samples are created using Taguchi (orthogonal) L25 array with four factors having 5 levels as shown in Table I.

TABLE I
FACTORS AND LEVELS OF THE TORQUE FUNCTION IN THE FIRST ITERATION SAMPLE FOR BOTH TYPES OF BULK SURFACE GEOMETRIES

Variable name	**Level**				
	1	2	3	4	5
$\tau(\theta_{0\%-25\%})$	0	50	100	150	200
$\tau(\theta_{25\%-50\%})$	0	50	100	150	200
$\tau(\theta_{50\%-75\%})$	0	50	100	150	200
$\tau(\theta_{75\%-100\%})$	0	50	100	150	200

The accuracy of the surrogate model using these 25 samples for both the flat and irregular bulk surface did not meet the stated criteria for the R^2 and $RMSE$. In addition, the error between the predicted values and the actual output of the additional confirmation samples were to high as shown by Figure 10 and 11.

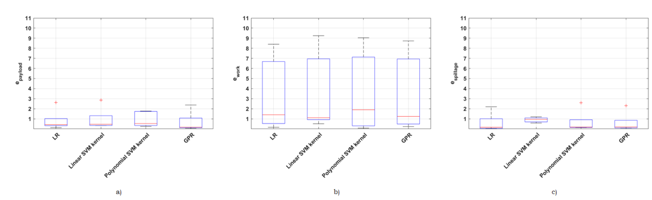

Fig. 10. Comparing simulated responses with their predicted response a) $\psi_{payload}$, b) ψ_{work} and c) $\psi_{spillage}$ for the flat bulk surface

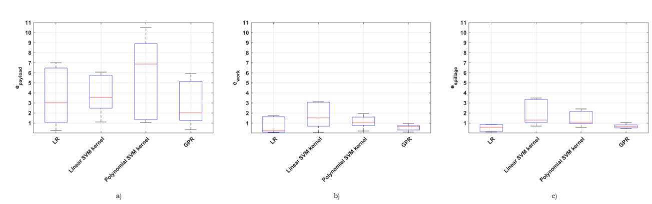

Fig. 11. Comparing simulated responses with their predicted response a) $\psi_{payload}$, b) ψ_{work} and c) $\psi_{spillage}$ for the irregular bulk surface

Therefore, the sample size is increased with an additional Taguchi design of 25 samples as shown in Table II.

TABLE II
FACTORS AND LEVELS OF THE TORQUE FUNCTION IN THE SECOND ITERATION SAMPLE FOR BOTH TYPES OF BULK SURFACE GEOMETRIES

Variable name	**Level**				
	1	2	3	4	5
$\tau(\theta_{0\%-25\%})$	100	125	150	175	200
$\tau(\theta_{25\%-50\%})$	100	125	150	175	200
$\tau(\theta_{50\%-75\%})$	0	25	50	75	100
$\tau(\theta_{75\%-100\%})$	0	25	50	75	100

The total of 50 samples meets all the stated criteria. The error between the predicted values and the actual output of the additional confirmation samples were also below the acceptable error of 5%. The LR model was found to be the most accurate regression model for the flat bulk surface and GPR for the irregular bulk surface.

Based on the finally developed surrogate model, GA is used to solve the optimization problem, thus, find the desired actuation function (i.e. desired torque function for the hybrid grab). Figure 12 presents the desired torque function found for the flat and irregular bulk surface. The x-axis displays the closing angle, θ, of the grab and the y-axis displays the level of torque, τ.

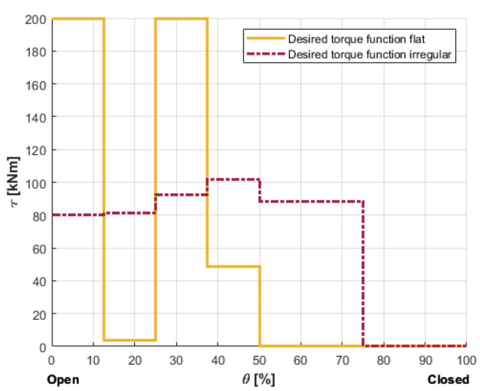

Fig. 12. Predicted desired torque function for the flat bulk surface using LR and irregular bulk surface using GPR

The desired torque functions show that relative high levels of torque are required at the first 50% of the closing angle, which results the optimum trade-off between maximizing the payload indicator, $\psi_{payload}$, maximizing the work indicator, ψ_{work} and maximizing the spillage indicator, $\psi_{payload}$. Table III shows the verification results of the predicted response of the desired torque. The relative error is $\leq 5\%$ for all predicted responses in Table III for both the flat and irregular bulk surface. Therefore, surrogate modeling combined with GA can be recommend to find the desired torque function including different bulk surface variability. However, different surrogate models apply to different types of bulk surface geometries, which is LR model for the flat surface and GPR for the irregular bulk surface as tested in this research.

TABLE III
COMPARING SIMULATED RESPONSE USING THE OPTIMAL SET WITH PREDICTED VALUES OF SURROGATE-MODELING-BASED OPTIMIZATION FOR THE IRREGULAR BULK SURFACE

Model	**LR**			**GPR**		
Parameter	$\psi_{payload}$	ψ_{work}	$\psi_{spillage}$	$\psi_{payload}$	ψ_{work}	$\psi_{spillage}$
Unit	[−]	[−]	[−]	[−]	[−]	[−]
Y Simulated response	3.01	0.94	0.94	2.30	0.88	1.00
Y' Predicted response	3.03	0.94	0.98	2.33	0.89	1.00
d Individual desirability	3.02	0.95	0.97	0.56	0.51	0.99
D Overall desirability	0.62			0.66		
$e = \left\lvert\frac{Y-Y'}{Y}\right\rvert 100$	0.37	0.77	2.71	1.29	0.32	0.02

B. Effect of Changing the Importance on the Desired Actuation Functions Found

As mentioned, the objectives in the optimization problem were considered equally important. In this subsection the effect of changing the importance, r_i, of different objectives on the torque function is investigated. Therefore, five scenario's are defined as shown in Table IV. Importance is chosen in the range from the least important value of 0.1 to the most important value of 10. The first scenario is considered as a reference case where equal importance is assigned to each objective.

TABLE IV
FIVE DIFFERENT SCENARIO'S CONSIDERING DIFFERENT IMPORTANCE FACTORS, r_i, FOR EACH OBJECTIVE

Scenario		**Importance**		
		$r_{payload}$	r_{work}	$r_{spillage}$
SC1	Equal importance	1	1	1
SC2	Maximum importance payload	10	0.1	0.1
SC3	Ignore spillage	10	10	0.1
SC4	Importance payload	7.5	2.5	0.1
SC5	Importance work	2.5	7.5	0.1

SC2 results in a torque function that reaches for the maximum torque level of 200 kNm for $0\% \leq \theta \leq 75\%$ for both the flat and irregular bulk surface. The levels of torque for $50\% \leq \theta \leq 100\%$ in SC1, SC3, SC4 and SC5 are approximately zero. This is because the grab is already full with bulk solid (i.e. the grab is outperforming its buckets), thus, $\psi_{payload}$ will have no or little increases but ψ_{work} will certainly increases as higher torque levels are applied for $50\% \leq \theta \leq 100\%$. Since this is a undesirable effect according to the stated objectives, the torque levels are nearly zero for $50\% \leq \theta \leq 100\%$. When spillage is ignored, i.e. SC3, the difference in predicted response is approximately 3% ($\approx$ 0.95 ton) for $\psi_{payload}$, 1% for ψ_{work} and 1% ($\approx$ 0.09 ton) for $\psi_{spillage}$ compared to SC1. Since the spillage objective has a relatively low influence on the found torque function and predicted response, a low importance value can be recommend for the spillage objective.

The different scenario's showed the effect of different importance values assigned to the objectives on the torque function. It is up to the designer or researcher to assign appropriate importance to the objectives based on their criteria or preferences.

VI. Exploring Hybrid Grab Concepts under Varying Operational Conditions

As the desired torque function is acquired for the flat and irregular bulk surface, hybrid grab concepts can be developed that can approximate this torque function or can follow the same trend with lower torque levels. Therefore, four hybrid grab concepts are developed for which the performance is evaluated using back-of-the-envelope calculations or by testing the hybrid grab concept in the co-simulation MBD-DEM environment. Figure 13 illustrates the four hybrid concepts: (I) NX grab SS, (II) NX grab CS, (III) NX grab RE and (IV) NX grab P.

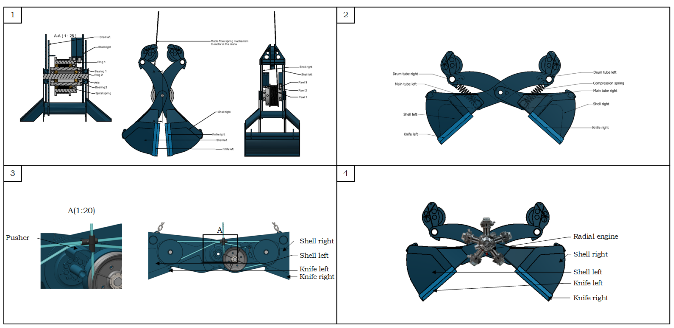

Fig. 13. Four hybrid grab concepts

A. NX grab SS

The first concept uses a spiral spring to store and released energy in the form of applying torque on the grab. By opening and closing of the grab the spiral springs gets tensioned. The performance and feasibility of this concept is determined based on the calculated mass of spiral spring for different materials. The total mass of the grab is an important performance indicator, increasing the mass results in less iron ore material to be grabbed for a defined crane capacity. For the flat bulk surface the work that is required to generate the desired torque function is 151.77 kJ and for the irregular bulk surface it requires 132.55 kJ of work. Thus, this amount of work needs to be stored in the spring and during the closing of the grab needs to be released to generate the desired torque function. The volume of the spiral spring that is needed to store that amount of work can be calculated according to Eq. (5).

$$W = \frac{V\sigma^2}{6E} \tag{5}$$

where V is the volume of the spring, σ is the allowable stress of the spring and E is the Young's modulus. Based on Eq. (5) the volume of the spring required to store the amount of work is calculated. Then, the mass of the spiral spring is calculated according to Eq. (6):

$$\rho = \frac{m_{spring}}{V} \tag{6}$$

where ρ is the density of the material used for the spiral spring and m_{spring} is the mass of the spiral spring. Commonly used material for a spiral spring is cold-rolled steel strip according to DIN 17222 [11]. Using this material the weight of the spiral spring is 358.91 kg for the flat bulk surface and 313.46 kg for the irregular bulk surface. Although this can be an acceptable mass for the spring, other materials might perform better. Using the Asbhy method [12] other spring material candidates are identified based on the minimum-weight criteria. For example, natural rubber will result in a spring mass of 2.38 kg for the flat bulk surface and 2.08 kg for the irregular bulk surface. However, besides the minimum-weight criteria additional considerations, i.e. availability of material, economical feasibility, recycling, need to be taken into account for selecting the spring material in this concept.

B. NX grab CS

The second concept (multiple) compression spring on each side of the grab for torque generation. Three configurations of the NX grab CS are investigated: (I) NX grab CS - DT and MT with impact force, (II) NX grab CS - VL and (III) NX grab CS - DT and MT with motor. The performance of these configurations is determined using the co-simulation MBD-DEM. Figure 14 shows the payload as a function of time for different configurations of the NX grab CS.

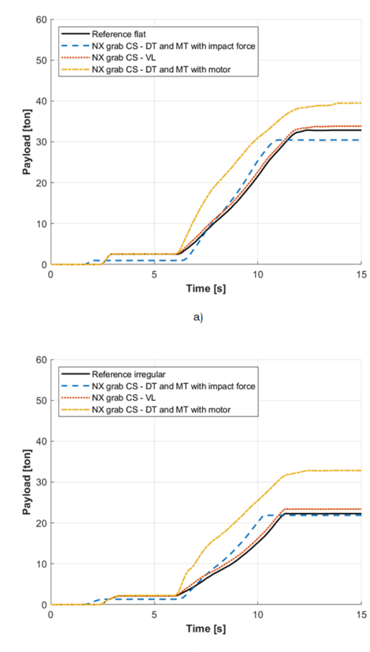

Fig. 14. Payload over time for different configurations of the NX grab CS for a) flat bulk surface and b) irregular bulk surface

The NX grab CS - DT and MT with motor shows the best result in terms of payload and unloading capacity under varying operational conditions. The NX grab CS - DT and MT with motor showed an additional increase of 20.2% in payload for the flat bulk surface and 47.4% for the irregular bulk surface compared to their references; equal to increase of 6.6 ton and 10.6 respectively. This resulted in an additional increase of 16.4% in unloading capacity for the flat bulk surface and 40.8% for the irregular bulk surface compared to their references. The NX grab CS - DT and MT with motor is able to maximize the payload with the possibility to become adaptive under varying operation condition, thus, allows for maintaining a consistent payload. The adaptiveness to varying operational conditions lies in using the spring locking mechanism and controlling the energy storage.

C. NX grab RE

The third concept uses the radial engine is powered by pressurized hydraulic fluid and transfer rotational kinetic energy to mechanical energy causing the axis of the grab to rotate. Radial engine, when powered by a mechanical source, can rotate in the reverse direction, and act as a pump to store energy in an accumulator. The described working principle can also be applied using pneumatic.

The performance and feasibility of this concept is determined based on specifications the radial engine must exhibited to generate the desired torque functions. The radial engine is a piston type engine. The speed at which a piston engine operates will usually depend on its size. The radial engine can be classified as a high-speed rotary engine. In the ideal situation, this radial engine can generate a maximum torque of 81.17 kNm calculated using the maximum values of power and angular velocity found in [13]. However, in reality this maximum torque value will never be reached as the torque descends after its peak due to the difficulty of forcing air into the engine. In addition, such an engine can weight approximately 3 tons, which is equal to approximately 25% of total mass of the NemaX grab (i.e. $m_{grab} \approx 12$ ton).

D. NX grab P

The fourth concept shows a bent steel plate, so-called pusher, placed at a fixed position above the main hinge. When the grab is lowered onto the bulk material and causes the closing rope to be redirected over. By redirecting the closing cables over the pusher a larger gear ratio is created. Thus, if you calculate the moment around the main hinge by multiplying the force of every cable times the arm you get a bigger gear ratio with a pusher. Figure 15 shows the payload as a function of time for different radii of the NX grab P.

As shown by the results, a maximum additional 0.6% increase in payload for both the flat and irregular bulk surface is observed. However, the NX grab P causes also a 2.3% decrease in unloading capacity for the flat bulk surface and 6.2% for the irregular bulk surface. Therefore, the increase in payload is outweighed by the decrease in unloading capacity.

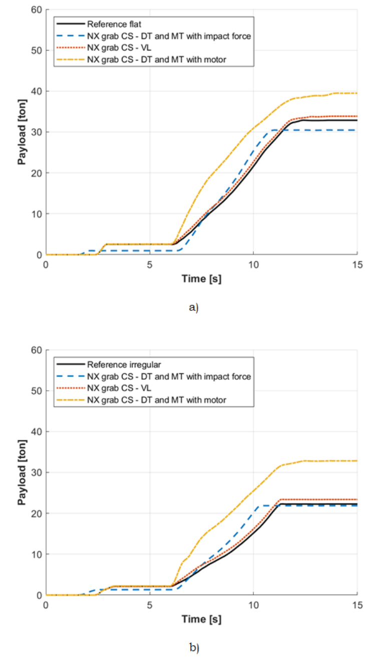

Fig. 15. Payload over time for different radii of the NX grab P for a) flat bulk surface and b) irregular bulk surface

VII. Conclusion

The main objective of this research was to develop and investigate hybrid grab concepts that maximize the payload with the possibility to become adaptive under varying operational conditions. The varying operational conditions included in this research is the bulk surface geometry; specifically a flat bulk surface and irregular bulk surface. The established hybrid grab design strategy was applied successfully to investigate, develop and test different hybrid grab concepts and find the desired torque function.

A optimization strategy for the desired torque function when varying operational conditions are included was developed and verified. However, it cannot be expected to provide a precise solution as the precision of the surrogate model is limited by many factors, including the initial Design of Experiments, initial sample size and the complexity of the original problem. The optimization strategy showed sufficient accuracy in predicting the desired torque function when multiple response and bulk surface geometry as varying operational condition are included. This allowed for obtaining the duration and level of extra torque to apply during the grabbing process that results in the desired grab performance. This optimization strategy can be applied to any type varying operational condition. According to the desired torque function, hybrid grab concepts are developed that can reduce the influence of varying operational conditions. The desired torque function showed how the hybrid grab should adapt with respect to the varying operational conditions.

The NX grab SS, NX grab CS, NX grab RE and NX grab P hybrid grab concepts are the results of following the design strategy. It is shown that every investigated hybrid grab concept has potential in terms of feasibility and approximating the desired torque function. The NX grab CS and NX grab P are more advanced in their design process due their performance evaluation in the co-simulation MBD-DEM, thus, are closer to be implemented in the NemaX grab design. Eventually, the NX grab CS - DT and MT with motor (one of the configurations of the NX grab CS) gave the best result in terms of payload and unloading capacity under varying operational conditions. The NX grab CS - DT and MT with motor showed an additional increase of 20.2% in payload for the flat bulk surface and 47.4% for the irregular bulk surface compared to their references; equal to increase of 6.6 ton and 10.6 respectively. This resulted in an additional increase of 16.4% in unloading capacity for the flat bulk surface and 40.8% for the irregular bulk surface compared to their references.

The NX grab CS - DT and MT with motor is able to maximize the payload with the possibility to become adaptive under varying operation condition, thus, allows for maintaining a consistent payload. The adaptiveness to varying operational conditions lies in using the spring locking mechanism and controlling the energy storage. The result of the design strategy applied for developing hybrid grab concepts can be used in further developments towards adaptive grabs.

Acknowledgment

The authors acknowledge the support of NEMAG B.V., The Netherlands. Their support is gratefully acknowledged.

References

[1] L. Scardua, J. Da Cruz, and A. Reali Costa, "Optimal control of ship unloaders using reinforcement learning," *Advanced Engineering Informatics*, vol. 16, no. 3, pp. 217–227, 2002.
[2] N. de Vries, "Design of grabs under operational conditions," *Delft University of Technology, 2020.MME.8452*, 2020.
[3] W. de Kluijver, "Rope grab design: a dem study on the closing mechanism of an iron ore pellet grab," *Delft University of Technology, 2014.TEL.7870*, 2014.
[4] A. van den Bergh, "Systematic design optimization of grabs handling cohesive bulk materials: Systematisch ontwerp optimalisatie van overslag grijpers voor cohesive bulk materialen," *Delft University of Technology, 2019.TEL.8363*, 2019.
[5] S. Lommen, "Virtual prototyping of grabs: Co-simulations of discrete element and rigid body models," *Delft University of Technology*, 2016, doi: PhD Thesis.
[6] M. Mohajeri, "Grabs and cohesive bulk solids - virtual prototyping using a validated co-simulation," 2021, doi: PhD Thesis.
[7] C. Xu and J. Zhu, "Parametric study of fine particle fluidization under mechanical vibration," *Powder Technology*, vol. 161, no. 2, pp. 135–144, 2006.
[8] M. Kunne, "A bio-inspired approach to grab design," *Delft University of Technology*, 2017.
[9] P. Jiang, Q. Zhou, and X. Shao, *Surrogate Model-Based Engineering Design and Optimization*. Springer, 2020.
[10] G. Derringer and R. Suich, "Simultaneous optimization of several response variables," *Journal of quality technology*, vol. 12, no. 4, pp. 214–219, 1980.
[11] H. Wittel, D. Jannasch, and D. Muhs, *Roloff/Matek machine-onderdelen: theorieboek*. SDU-Academic Service, 2013.
[12] M. Ashby and D. Cebon, "Materials selection in mechanical design," *Le Journal de Physique IV*, vol. 3, no. C7, pp. C7–1, 1993.
[13] P. Breeze, "Chapter 3 - types of reciprocating engine," in *Piston Engine-Based Power Plants*. Academic Press, 2018, pp. 21–33.